34th Annual International Conference of the IEEE EMBS
San Diego, California USA, 28 August - 1 September, 2012

A Robotic Interface to Train Grip Strength, Grip Coordination and Finger Extension Following Stroke

Hamed Kazemi *Student Member, IEEE*, Robert E. Kearney, *Fellow, IEEE* and Theodore E. Milner, *Member, IEEE*

***Abstract*— A two degree of freedom robotic interface was developed to assist with rehabilitation of three hand impairments following stroke: reduced grip strength, reduced finger extension, and loss of dexterity due to the lack of coordination between finger and wrist muscles. The design and performance characteristics of this interface, which takes advantage of an FPGA-based real-time platform, are discussed. The robotic interface is able to accurately render elastic and viscous loads. Preliminary trials with healthy subjects demonstrate the use of the device.**

I. INTRODUCTION

The combination of intensive task-specific exercise and general aerobic exercise is still the most effective approach to the rehabilitation of motor function after stroke [1]. Nevertheless, 15-30% of stroke survivors face permanent disability. Research in robot-assisted therapy aims to develop alternative and better training strategies and therapies. Robots can assist therapists by providing consistent, precise therapy for long periods without fatigue. More stroke survivors could receive therapy if effective robots were mass produced. Since robots are programmable, exercises could be tailored to individual need and level of impairment. In addition, they could be used as quantitative assessment tools to measure the kinematics and kinetics of the exercise to provide real time feedback or track changes over the course of therapy. Several robotic interfaces have been developed for rehabilitation of the upper extremity in the past 15 years (see [2] for a review), mostly aimed at shoulder and elbow movements.

Hand impairments persisting after stroke include reduced grip strength, spasticity, loss of dexterity, impaired coordination of fingertip forces, reduced finger and wrist extension, impaired coordination of finger joints and impaired ability to move fingers independently [3]. Improving hand function in stroke patients is necessary to enable them to carry out activities of daily living and lead an independent life. A recent review of hand-targeted robotic interfaces examined 9 end-effector based devices and 21 exoskeletons and concluded that there is preliminary but promising evidence that robot-assisted rehabilitation of hand function is effective [4]. However, most current devices suffer from limited force and torque capacity. In addition, most devices that target the hand and wrist, train only one aspect of hand function (e.g. grasping), and ignore others. Moreover, only about 25 percent of the hand training robots have been clinically tested [4]. Therefore, there is a continued need for developing effective hand training devices and evaluating them clinically.

*Supported by the Canadian Institutes of Health Research (CIHR)
Hamed Kazemi is with the Department of Biomedical Engineering, McGill University, Montreal, H3A 2B4 Quebec, Canada
(e-mail: hamed.kazemi@mail.mcgill.ca).
Robert E. Kearney is with the Department of Biomedical Engineering, McGill University, Montreal, H3A 2B4, Quebec, Canada
(e-mail: robert.kearney@mcgill.ca).
Theodore E. Milner is with the Department of Kinesiology and Physical Education, McGill University, Montreal, H2W 1S4 Quebec Canada
(e-mail: theodore.milner@mcgill.ca).

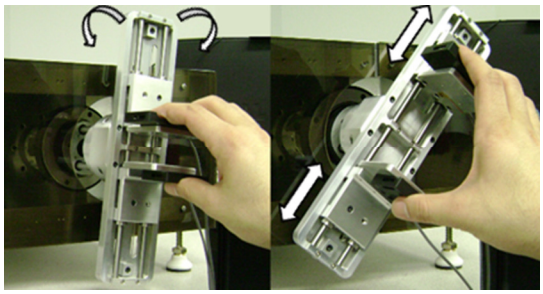

Figure 1. A two DOF hand robot. Arrows indicate opening/closing and rotational movements of the end-effector.

This paper describes the design, construction and performance evaluation of a robotic interface developed to assist with the rehabilitation of three impairments following stroke. Pilot data involving measurements obtained from 8 healthy subjects using the robotic interface are presented.

II. DESIGN AND CONSTRUCTION

A. Concept

The creation of an appropriate rehabilitation device involves identifying impairments of the contralesional hand and selecting exercises that target these impairments. The underlying premise is that repetition of appropriate exercises will reduce the impairment by facilitating functional neuroplasticity and promoting motor learning.

B. Rational and Design Requirements

The goal of this study was to address three hand impairments that persist after stroke: reduced grip strength (muscle weakness), reduced finger extension, and loss of dexterity due to the lack of coordination between finger and wrist muscles. Therefore, the design goal was to build a robotic interface that would address these impairments by:

1. Improving grasping function and finger flexion strength by using various resistive loads during exercises.
2. Increasing strength of finger extensors and range of motion using resistive loads in finger extension exercises.
3. Improving coordination of the wrist and fingers, which is critical for controlling hand orientation and performing various activities of daily living such as turning knobs or unscrewing lids. The focus will be on grip force

978-1-4577-1787-1/12/$26.00 ©2012 IEEE

regulation during grasping and forearm twisting under various load conditions.

These functional requirements led to the following design requirements:

1. The device must have two active degrees of freedom (DOF): a translational DOF for hand opening/closing movements (grasping and finger extension) and a rotational DOF for forearm supination/pronation (twist).
2. The device must have sufficient force and torque capacity to render a variety of load characteristics and provide strength training (The average pinch force generated by healthy adults older than 50 years has been reported to be less than 120 N [5]).
3. The device must be able to measure hand aperture, forearm rotation, force exerted by the thumb and other fingers and the wrist torque.
4. The bandwidth of the system (relating commanded current input to generated torque output) must be broader than the range of frequencies present during hand movement (the maximum frequency of voluntary hand movements is less than 5 Hz, although involuntary movements such as physiological tremor can be as high as 8-12 Hz).

C. Construction

The hand robot was designed with a jaw that opens and closes to train grasping functions and a rotational DOF to provide supination/pronation movement of the forearm to train coordination of grasping with twisting (see Fig. 1).

The device is driven by two DC brushed motors (RE 75, 250W, Maxon, Switzerland) which provide opening and closing movement along a radial axis and rotational movement about the horizontal axis of the end-effector. One DC motor drives a linear actuator/guideway module (Schneeberger Linear Technology) through a pair of reduction pulleys (1:2) which translate the rotation to horizontal movement. This module is coupled to a mechanism incorporating linear and rotational bearings, 5 pulleys and a drive cable, which decouples the rotation of the end-effector and translates the horizontal movement to opposing movement of two end-effector finger plates.

A second DC motor drives the rotational axis of the end-effector through a second pair of reduction pulleys (1:4). As safety precautions, hard mechanical stops limit the range of movement of the device and force, torque and position limits are implemented in the control program. Interchangeable fixtures can be mounted on the interface to train a variety of grips, including cylindrical grip, five, four or three finger chuck, fingertip pinch and key grips.

The range of motion (ROM) of the robot is ±180º along the rotational DOF and 15-150 mm along the translational DOF. The continuous force capacity of the translational DOF is 200 N and the continuous torque capacity is 5 Nm for the rotational DOF.

Optical encoders (E6, USDigital, Washington) mounted on the motor shafts read the angle of the motors with a resolution of 10000 counts per revolution which is then mapped to the rotational and translational displacements of the end-effector based on the kinematic transformation. The resolution for the rotational DOF is 0.009 deg and 0.008 mm for the translational DOF. The upper and lower jaws of the interface are instrumented with strain gauges to measure the normal grip force exerted by the thumb and the fingers with a resolution of 0.012 N. The device also has a torque sensor with a resolution of 0.011 Nm to measure the torque exerted by the user.

An embedded monitoring and control system from National Instruments (CompactRIO-9074), which combines a reconfigurable field-programmable gate array (FPGA) and a real-time processor, was used for computations and communication. The FPGA system handles all position calculations from encoders, force and torque calculations, time-critical haptic rendering along with analog commands to the motors with loop rates of up to 100 kHz. The host computer acts as a communication interface and also provides visual feedback. DMA FIFO (Direct Memory Access First in First Out) architecture was used for data transfer from the reconfigurable CompactRIO device to the host computer. Data were sampled at 1 kHz with ADC resolution of 16 bits. Anti-aliasing filtering with a cut-off frequency of 100 Hz was performed. The hardware platform setup is shown in Fig. 2.

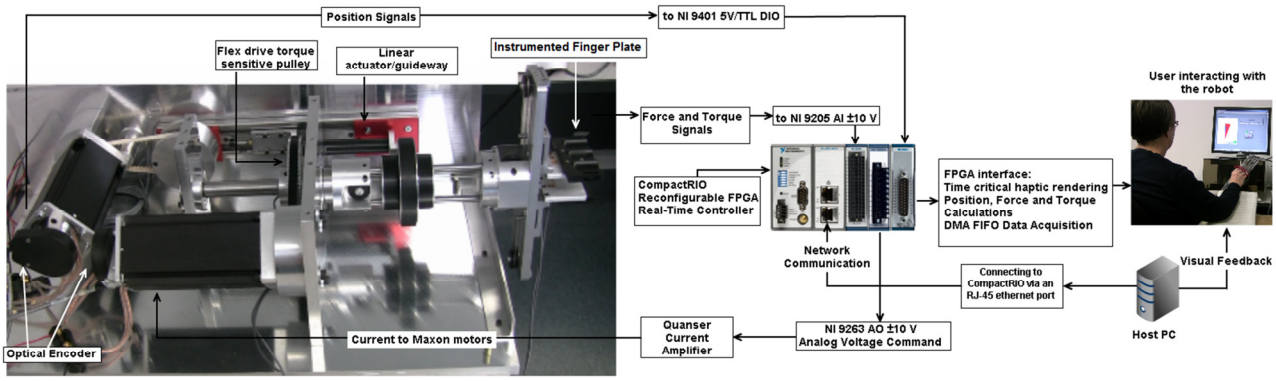

Figure 2. Hardware platform setup with real time FPGA system. The FPGA system performs position, force and torque calculations from sensors as well as time-critical haptic rendering and sends analog commands to the motors via the current amplifiers. A simple impedance controller, using LabVIEW FPGA (NI, v.8.6.1), renders a virtual spring and damper. The host PC communicates with the FPGA over the network to achieve data transfer and provides visual feedback to the user. Mechanical components of the hand robot are also shown.

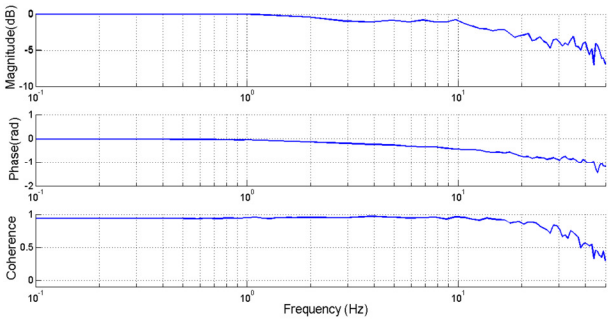

Figure 3. Frequency response along the rotational DOF.

III. PERFORMANCE EVALUATION

A. Frequency Response

To assess the dynamic performance of the interface and estimate its frequency response, the current to the motor was controlled and the output torque was measured while the end-effecter was locked. A Gaussian-distributed pseudorandom command with bandwidth of 0-50 Hz and peak to peak amplitude of 0.5 A (corresponding to a torque of 1 Nm) was applied as the command input. The computed frequency response of the system is shown in Fig. 3. The coherence squared was greater than 0.80 up to 28 Hz, suggesting that the response was linear up to that frequency. The gain was flat at low frequencies and then rolled off down to -3 dB by about 21 Hz. The phase lag was flat at low frequencies then slowly increased. Therefore, the open loop bandwidth of the device for rotation is 21 Hz. Also, the open loop bandwidth for translation was estimated to be 19 Hz.

The closed loop bandwidth of the unconstrained interface was estimated from the frequency response between the desired position input and the measured position for a randomly varying command. It was DC to 14 Hz for translation and DC to 16 Hz for rotation. Bandwidths of 14 Hz and 16 Hz are more than adequate as these are greater than the range of frequencies present during hand movement.

B. Haptic Control Architecture

A simple impedance controller was implemented in LabVIEW FPGA (NI, v. 8.6.1) to render a virtual environment taking the form of a spring and damper. The

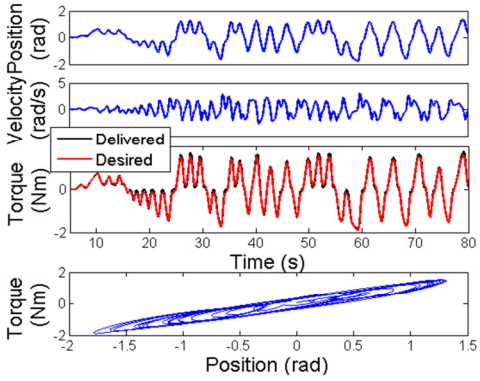

Fig 5. Rendering of stiffness of 1Nm/rad and damping of 0.15 Nm.s/rad in rotation during 80 sec of user interaction with the robot.

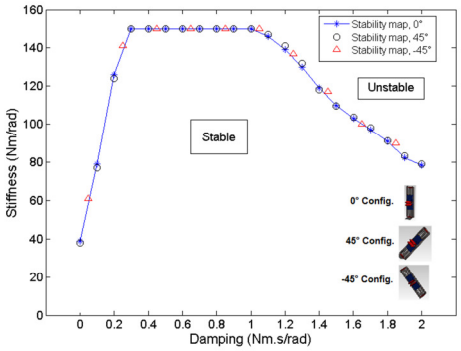

Figure 4. Stability map of the imepdence controller along the rotational DOF in three different configurations.

controller used the differences between the changes in desired position and actual end-effector position to generate the desired force/torque command by multiplying the detected change in motion by the desired virtual environment impedance.

To find the stability map, a step change in the commanded position of 10 deg for the rotational DOF and 15 mm for the translational DOF was applied to the unconstrained interface and the response was monitored for any sign of instability such as undamped oscillation or resonance. For each damping value, the stiffness was increased until instability occurred. A stiffness range to 150 Nm/rad and damping range to 2 Nm.s/rad were explored. The map of gains for which the controller remained stable along the rotational DOF is shown in Fig. 4. The experiment was repeated for three different end-effector configurations. It is important to note that these experiments were performed when no load was attached nor any user interacted with the end-effector. The stability map shown in Fig. 4 would likely change when a user holds the device.

The sensor resolution (Δ), inherent coloumb (c) and viscous (b) friction in the system and sampling period of the controller (T) are known to affect the stability of haptic control systems [6]. To ensure that the system remains passive, the maximum stiffness to be rendered cannot exceed the minimum of $2b/T$ and $2c/\Delta$ [6].

To demonstrate that the haptic rendering algorithm produced the specified stiffness and damping, an experiment was conducted in which the user interacted with the device along the rotational DOF (free movement task). The impedance controller was set to deliver stiffness of 1 Nm/rad and damping of 0.15 Nm.s/rad. Fig. 5 shows the position and the velocity profile as well as the desired (computed by multiplying desired impedance by position and velocity) vs.

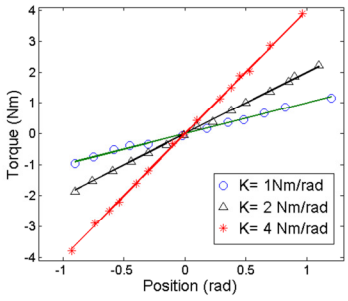

Fig 6. Torque command and measured torque for three stiffness values.

TABLE 1. PERFORMANCE COMPARISON WITH HAPTIC KNOB [7] AND REHAPTICKNOB [8]

Device	Haptic Knob		ReHapticKnob		Current robot	
DOF	Translation	Rotation	Translation	Rotation	Translation	Rotation
Range of Motion	30-150 mm	±180	30-200mm	±159	15-150mm	±180
Static friction	9 N	0.02 Nm	6 N	< 0.4 Nm	5.4 N	0.08 Nm
Maximum continuous force	30 N	-	80 N	-	200 N	-
Maximum continuous torque	-	1.5 Nm	-	4 Nm	-	5 Nm
Closed loop position bandwidth	-	-	6.6 Hz	7.6 Hz	14 Hz	16 Hz
Update rate of the controller	100 Hz		1 kHz		100 kHz	

delivered torque. The controller closely tracked the commanded elastic and viscous torque. In another experiment, the user was asked to hold the end-effector at different positions while the robot exerted a spring load. The measured torque accurately matched the desired torque for stiffness values from 1 to 4 Nm/rad as shown in Fig. 6.

IV. PRELIMINARY TRIALS IN HEALTHY SUBJECTS

Several exercises and assessment protocols were developed for the hand-robot. For example, Fig 7 shows the position, load torque and grip force during a grip coordination exercise performed by a healthy subject. The task involved grasping the end-effector and rotating it to a target position while the robot exerted a spring load torque. As can be seen, the torque increases as the rotation angle increases forcing the subject to modulate grip force as the angle of rotation changes to avoid rotational slip. Eight healthy individuals (all right handed, mean age 24.1 years) performed 10 trials of the grip coordination exercise. The target position and the torsional spring stiffness were set to 20 deg and 0.015 Nm/deg, respectively. The ratio of maximum grip force to maximum load torque is shown in Fig. 8. This measure, which is an indicator of scaling of grip force with respect to load torque, was consistent (did not differ significantly across subjects) and may be used to study the differences between impaired and healthy grip coordination behaviour.

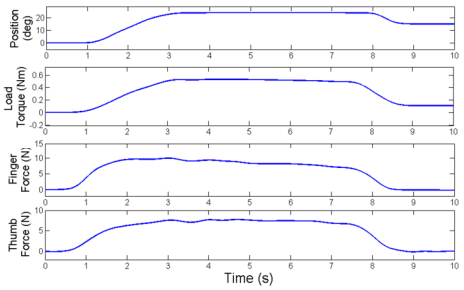

Figure 7. Position, load torque and grip force during a grip coordination task performed by a healthy subject.

V. CONCLUSION

We have developed a novel 2 DOF robotic interface which is capable of delivering elastic and viscous loads over a large range for training hand function. It can also serve as an assessment tool by tracking physical measures of grip strength, wrist torque and hand range of motion. Compared to other hand robots, in particular, Haptic Knob [7] and ReHapticKnob, [8] which share some of the same design concepts, this interface has higher force and torque capacities. Table 1 compares the performance measures of all three devices. The current device also has less friction and thus, better back drivability. Moreover, the bandwidth of the current system is higher.

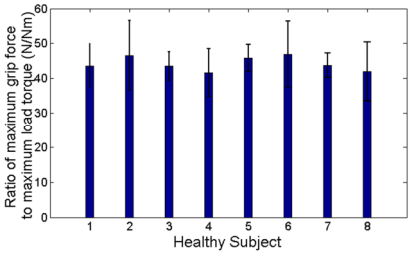

Figure 8. Ratio of maximum grip force to maximum load torque during grip coordination in 8 healthy subjects.

ACKNOWLEDGMENT

We thank S. De Serres, A. Gosline, A. Sato, D. Pavlasek and B. Thomson, from McGill who all contributed to the design of this robotic device. Also, HK thanks O. Lambercy from ETH-Zurich for his valuable insights on this project.

REFERENCES

[1] M.A. Dimyan and L.G. Cohen, "Neuroplasticity in the context of motor rehabilitation after stroke," *Nat Rev Neurol*, 2011. 7(2): 76-85.

[2] G. Kwakkel, B. J. Kollen and H. I. Krebs, "Effects of robot-assisted therapy on upper limb recovery after stroke: a systematic review," *Neurorehabil Neural Repair*, 2008. 22(2): pp. 111-21.

[3] P. Raghavan, , "The nature of hand motor impairment after stroke and its treatment". *Curr Treat Options Cardiovasc Med*, 2007. 9(3): pp.221-8.

[4] Balasubramanian, S., Klein, J. and Burdet, E., "Robot-assisted rehabilitation of hand function" *Curr Opin Neurol*, 2010. 23(6): pp. 661-70.

[5] C.A. Crosby, M.A. Wehbé, "Hand strength: Normative values", *The Journal of Hand Surgery*, 1994, 19(4),: pp. 665-670.

[6] N. Diolaiti, G. Niemeyer, F. Barbagli, and J. K., Jr. Salisbury, "Stability of Haptic Rendering: Discretization, Quantization, Time Delay, and Coulomb Effects," *IEEE Trans. Rob.*, 2006. 22(2): pp. 256–268.

[7] O. Lambercy, L. Dovat, R. Gassert, E. Burdet, C.L. Teo and T. Milner, "A Haptic Knob for Rehabilitation of Hand Function," *IEEE Trans. Neural Syst. Rehabil. Eng.* 2007. 15(3): pp. 356-366.

[8] J.C. Metzger, O. Lambercy, D. Chapuis, and R. Gassert, "Design and characterization of the ReHapticKnob, a robot for assessment and therapy of hand function," *Intelligent Robots and Systems (IROS), IEEE/RSJ Int. Conf.* 2011: p. 3074 - 3080